



# Adhesion force of polymeric three-dimensional microstructures fabricated by microstereolithography

Dongmin Wu, Nicholas Fang, Cheng Sun, and Xiang Zhang<sup>a)</sup>

*Department of Mechanical and Aerospace Engineering, University of California at Los Angeles, 420 Westwood Plaza, Los Angeles, CA 90095*

(Received 19 June 2002; accepted 27 September 2002)

The adhesion between microstructures represents a great challenge in reliability of polymeric three-dimensional structures fabricated by microstereolithography ( $\mu$ SL). During the evaporative releasing, the capillary force of the solvent causes the deformation and adhesion of the fabricated beams. We present a method to determine the adhesion force of polymeric microstructures fabricated by  $\mu$ SL. The test structures with parallel beams were fabricated and released from the liquid resin via evaporation. By measuring the relationship between the adhesion length and the geometry of the beams, the adhesion force between two 1,6-hexanediol diacrylate (HDDA) polymeric parallel beams is determined as  $\gamma = 72 \pm 5$  mN/m. This simple method and the determined adhesion force provide a key in designing reliable polymeric microelectromechanical systems in preventing the stiction problem. © 2002 American Institute of Physics. [DOI: 10.1063/1.1522825]

Microstereolithography ( $\mu$ SL), evolved from the traditional rapid prototyping technology, is introduced to fabricate truly three-dimensional (3D) polymeric and ceramic microstructures for microelectromechanical systems (MEMS) devices.<sup>1,2</sup> This promising technique provides the designers with a simple approach to converting the computer aided designed (CAD) model into truly 3D microcomponents and devices with complex geometry. In  $\mu$ SL, the microstructures are fabricated by UV light localized photopolymerization of the liquid resin, in a layer-by-layer manner. A 3D CAD model is sliced into a series of two-dimensional (2D) sections, and each of the sections is then used to direct the localized UV beam exposure to form a specific layer. By stacking the layers, one can fabricate 3D complex structures designed by the CAD model. Using two photon polymerization, the resolution of  $\mu$ SL has recently been increased from several microns to sub-microns.<sup>3,4</sup> The  $\mu$ SL technique provides a manufacturing method for truly 3D MEMS devices. This technique also can fabricate microstructures with many functional materials<sup>5</sup> other than those used in integrated circuit industry for MEMS. Compared with the traditional 2D or 2.5D silicon micromachining technique, the capability of fabricating complex 3D microstructures along with very broad materials selections makes  $\mu$ SL especially attractive in realizing applications of 3D MEMS devices, such as miniature sensors and actuators, by integrating the microelectronics and micromechanical machines. Among them, one can find the successful applications of  $\mu$ SL in microfluidic systems,<sup>6</sup> optical waveguides,<sup>7</sup> and 3D photonic band gap structures.<sup>8</sup>

One of the key factors that influences the performance and reliability of MEMS devices is the undesired adhesion between the microstructures during fabrication or during device operation. In macroscale devices, the adhesion problem is usually less significant because the elastic restoring force

of the mechanical structure can be much higher than the adhesion force. However, in microscale, the adhesion force may be strong enough to cause the permanent distortion of the microstructures and the failure of the devices. This phenomenon is known as “stiction problem” in silicon micromachining.<sup>9</sup> For the same reason, and because the Young’s modulus of the polymeric material is smaller than silicon, the stiction problem is even more severe in  $\mu$ SL fabricated 3D polymeric structures. It is therefore important to characterize the adhesion force between the polymeric structures to provide a better design for the MEMS devices. In this letter, we present a method to determine the adhesion force which is characterized by the surface energy between the 3D structures fabricated by  $\mu$ SL.

Figure 1 shows the test structure designed to measure the adhesion force between polymeric microstructures. Because the adhesion between the parallel beams is of interest, the supporting post is designed high enough to avoid the influences of the substrate. After  $\mu$ SL fabrication, the 3D structure is rinsed by solvent to remove the unpolymerized resin and then released by solvent evaporation. Figure 1(b) illustrates the mechanism of the adhesion phenomenon during evaporation drying. The beams are distorted by capillary force from the solvent captured between them. The beams will keep adhering even after drying, if the mechanical restoring force is smaller than the adhesion force between the beams. We define the adhesion length  $2x_s$  as the section where two beams contact.

An analytical model was developed previously for the stiction between planar polysilicon beam and the silicon substrate in the silicon surface micromachining.<sup>10,11</sup> We use a similar approach to analyze our 3D polymer structures and derive the adhesion length  $2x_s$ , as

$$2x_s = l \left[ 1 - \left( \frac{128 E h^2 l^3}{5 \gamma_s l^4} \right)^{1/4} \right], \quad (1)$$

where  $E$  is the Young’s modulus of polymer,  $\gamma_s$  the adhesion

<sup>a)</sup>Electronic mail: xiang@seas.ucla.edu

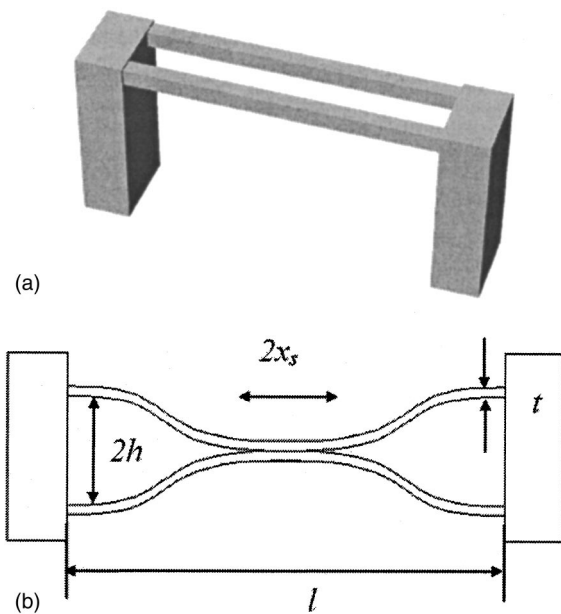


FIG. 1. Schematic of the micro-beam structures used to determine the adhesion force. (a) 3D model of the designed beams suspended on two posts on a silicon substrate. (b) The beams are adhered during evaporation drying by the capillary force of liquid solvent and stay adhered afterwards if the elastic restoring force is not enough to overcome the adhesion force (top view).

force (per unit length of the contact length) between polymer surfaces,  $l$  is the total beam length,  $2h$  is the spacing between parallel beams, and  $t$  is the beam width. According to Eq. (1), the adhesion length  $2x_s$  changes linearly with the geometry factor  $F = (h^2 t^3)^{1/4}$ . At the critical geometry  $F_d$ , the adhesion length equals zero, which means no stiction occurs even though the capillary force may bring the beams in contact with each other during the releasing process. We define the length of the beam at this critical geometry as detachment length  $l_d$ , in Eq. (2):

$$l_d = \left( \frac{128E}{5\gamma_s} \right)^{1/4} (h_d^2 t_d^3)^{1/4} = \left( \frac{128E}{5\gamma_s} \right)^{1/4} F_d. \quad (2)$$

When the beam length is larger than  $l_d$ , adhesion likely occurs. When the beam length is smaller than  $l_d$ , no adhesion occurs. The latter is due to the fact that as the beam length becomes smaller, the elastic restoring force increases for the same deformation of the beams and prevents permanent adhesion of beams. The  $l_d$  is related only to the geometry factor  $F_d$  of the test structure, the Young's modulus  $E$  and adhesion force  $\gamma_s$  of the polymer beams. With known Young's modulus of the  $\mu$ SL fabricated polymer beams, which is measured in previous study,<sup>12</sup> one can determine the adhesion force  $\gamma_s$  from Eq. (1) or (2).

The test structures are fabricated by a  $\mu$ SL system.<sup>13</sup> The UV curable resin is a mixture of 1,6-hexanediol diacrylate (HDDA) and 5 wt% benzoin ethyl ether as photoinitiator. The optimized exposure dose is 200 mJ/cm<sup>2</sup> with the UV wavelength at 365 nm. After fabrication, the test structures are prepared by the post processes, which include rinsing in a solvent, post-curing in the UV oven (Zeta™ 7200, Loctite), and releasing through evaporation at room temperature. Specifically, the mercury lamp is used as the UV light source for the post-curing process. The post-curing is performed by

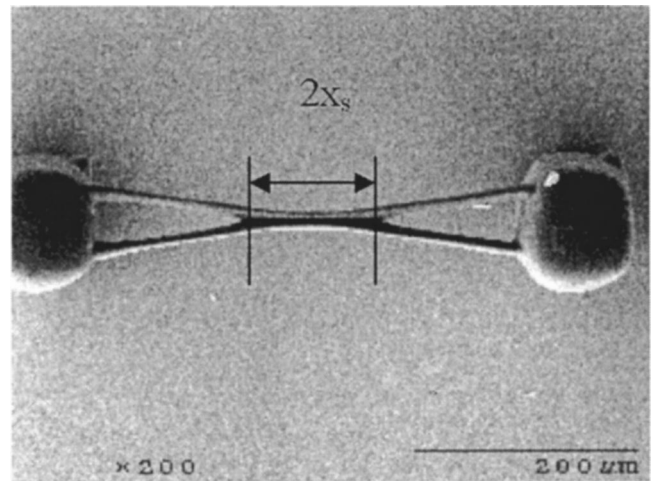


FIG. 2. N-SEM top view of suspended beams, released by evaporation. The beam length is 412  $\mu\text{m}$ , spacing is 50  $\mu\text{m}$ , thickness is 20  $\mu\text{m}$ , and the width is 9  $\mu\text{m}$ . The adhesion length  $2x_s$  measured is about 124  $\mu\text{m}$ .

placing the test structure in the oven for 1 min with a UV irradiation intensity of 50 mW/cm<sup>2</sup>. The final structures were observed and measured under environmental scanning electron microscopy (N-SEM).

Figure 2 is the N-SEM picture of a test beam structure after solvent evaporation. The picture shows that the beams adhere to each other about  $2x_s = 124 \mu\text{m}$  at the center part. In order to study the relationship between the adhesion length and the beam geometry from which the adhesion force  $\gamma_s$  can be determined, a group of test structures with same beam length and spacing, but different widths, were fabricated. After releasing these structures, the adhesion lengths  $2x_s$  were obtained by N-SEM. Figure 3 shows the experimental data of adhesion lengths as a function of geometry factor  $F$ . It is observed that the adhesion length is linearly dependent on  $F$ , which is in good agreement with the analytical model according to Eq. (1). By extrapolating the fitting curve in Fig. 3 to the point where  $x_s = 0$ , the critical value of the geometry factor  $F_d = 21.5 \mu\text{m}^{5/4}$  is obtained and then, the detachment length  $l_d = 525 \mu\text{m}$  is defined as the length of the beam at this critical geometry. This has been

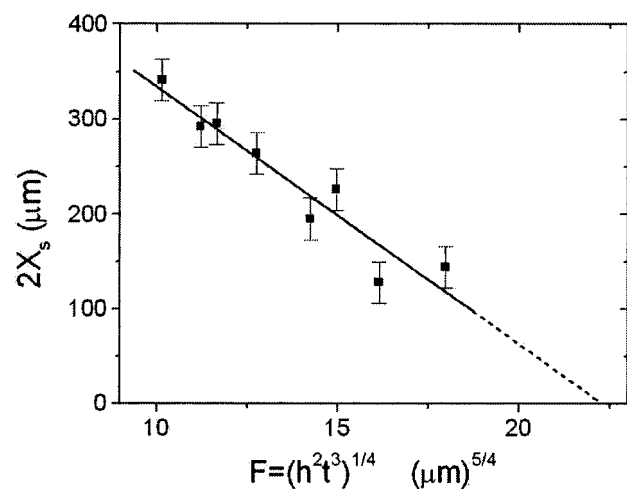


FIG. 3. Dependence of the adhesion length  $2x_s$  on geometrical factor  $F$ . The total beam length is 525  $\mu\text{m}$ . The data are fitted linearly to extrapolate the critical geometrical factor  $F_d$ .

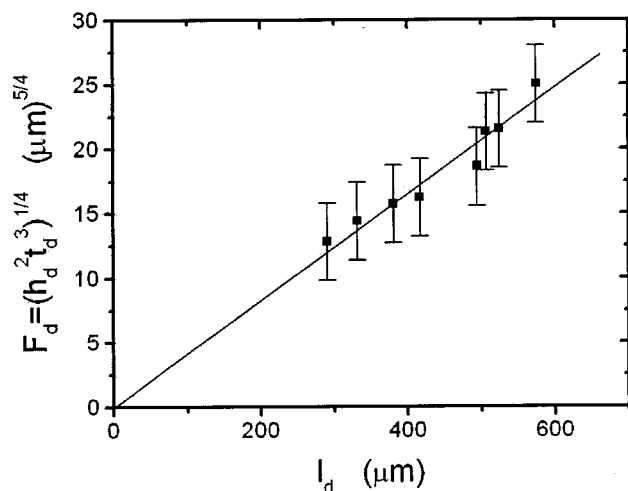


FIG. 4. Relationship of the detachment length versus  $F_d = (h_d^2 t_d^3)^{1/4}$  of the test structures. The data of  $F_d$  are from the fitting parameter in Fig. 3 at zero adhesion length.

experimentally verified by successfully released beams with the same geometry factor by shorter length. With a set of structures at various total beam lengths, we obtain the values of  $F_d = (h_d^2 t_d^3)^{1/4}$  corresponding to different detachment lengths  $l_d$ , shown in Fig. 4. The linear relationship is found between the detachment length  $l_d$  and  $F_d$ , which again confirms the validity of the model for beams at different geometries. According to Eq. (2), the slope in the linear fitting in Fig. 4 should be  $(5\gamma_s/128E)^{-1/4}$ . Atomic force microscopy (AFM) measurement of Young's modulus of HDDA ( $E = 930$  MPa) beams fabricated by  $\mu$ SL was performed in an earlier work.<sup>12</sup> With measured Young's modulus of HDDA beams ( $E = 930$  MPa) and the slope from Fig. 4, we found the adhesion force  $\gamma_s$  for HDDA as  $72 \pm 5$  mN/m.

In summary, we present a method to determine the adhesion force of polymer microstructures fabricated by microstereolithography. The linearity of the curve (Figs. 3 and 4) is in good agreement with the theoretical model. It should be further noted that the linearity between  $l_d$  and  $F_d$  also

suggests the adhesion force  $\gamma_s$  measured is the intrinsic property of polymeric microstructures and is independent of the beam geometries. Compared with other methods, such as the peel-off test and AFM measurement,<sup>14</sup> this approach is much simpler because it only requires the measurement of the geometry of the test structures. This method and the measured adhesion force  $\gamma_s$  provide a key in the designing of 3D microstructures in  $\mu$ SL to reduce and prevent the stiction problem and improve the reliability of MEMS devices.

This work is supported partially by the Department of Defense Multidisciplinary University Research Initiative (MURI) under Grant No. N00014-01-1-0803, Office of Naval Research (ONR) Young Investigator Award under Grant No. N00014-02-1-0224, and the National Science Foundation (NSF) CAREER Award under Grant No. DMI-0196395.

<sup>1</sup>K. Ikuta and K. Hirowatari, *Proceedings of the IEEE International Workshop on Micro Electro-Mechanical Systems (MEMS'93)* (IEEE, New York, 1993), pp. 42–47.

<sup>2</sup>C. Sun, N. Fang, and X. Zhang, *Sens. Actuators A* (accepted for publication).

<sup>3</sup>S. Kawata, H.-B. Sun, T. Tanaka, and K. Takada, *Nature (London)* **412**, 697 (2001).

<sup>4</sup>X. Zhang, X. N. Jiang, and C. Sun, *Sens. Actuators* **77**, 149 (1999).

<sup>5</sup>C. Sun, N. Fang, and X. Zhang, *J. Appl. Phys.* **92**, 4796 (2002).

<sup>6</sup>K. Ikuta, K. Hirowatari, and T. Ogata, *Proceedings of the International Conference on IEEE Micro Electro-Mechanical Systems* (IEEE, New York, 1994), pp. 1–6.

<sup>7</sup>S. Maruo, K. Ikuta, and T. Ninagawa, *Technical Digest, 14th IEEE International Conference on Micro Electro-Mechanical Systems (MEMS 2001)*, Piscataway, NJ (IEEE, New York, 2001), pp. 151–154.

<sup>8</sup>H.-B. Sun, S. Matsuo, and H. Misawa, *Appl. Phys. Lett.* **74**, 786 (1999).

<sup>9</sup>Chang-Jin Kim, John Y. Kim, and Balaji Sridharan, *Sens. Actuators A* **64**, 17 (1998).

<sup>10</sup>C. H. Mastrangelo and C. H. Hsu, *J. Microelectromech. Syst.* **2**, 33 (1993).

<sup>11</sup>C. H. Mastrangelo and C. H. Hsu, *J. Microelectromech. Syst.* **2**, 44 (1993).

<sup>12</sup>E. Manias, J. Chen, N. Fang, and X. Zhang, *Appl. Phys. Lett.* **79**, 1700 (2001).

<sup>13</sup>C. Sun, N. Fang, and X. Zhang, *Proceedings of the 2001 ASME International Mechanical Engineering Congress and Exposition, MEMS* (New York, 2001), Vol. 3, pp. 813–818.

<sup>14</sup>A. El Ghzaoui, *J. Appl. Phys.* **85**, 1231 (1999).